PCCP

Accepted Manuscript

This is an *Accepted Manuscript*, which has been through the Royal Society of Chemistry peer review process and has been accepted for publication.

Accepted Manuscripts are published online shortly after acceptance, before technical editing, formatting and proof reading. Using this free service, authors can make their results available to the community, in citable form, before we publish the edited article. We will replace this *Accepted Manuscript* with the edited and formatted *Advance Article* as soon as it is available.

You can find more information about *Accepted Manuscripts* in the Information for Authors.

Please note that technical editing may introduce minor changes to the text and/or graphics, which may alter content. The journal's standard Terms & Conditions and the Ethical guidelines still apply. In no event shall the Royal Society of Chemistry be held responsible for any errors or omissions in this *Accepted Manuscript* or any consequences arising from the use of any information it contains.

ROYAL SOCIETY OF CHEMISTRY

www.rsc.org/pccp

Polarization dressed multi-order Fluorescence of Pr^{3+}:Y_2SiO_5

Ruimin Wang[1,a)], Chengjun Lei[1], Changbiao Li[1], Huayan Lan[1], Huaibin Zheng[1], Min Xiao[2], and Yanpeng Zhang[1,b)]

[1]*School of Science & Key Laboratory for Physical Electronics and Devices of the Ministry of Education & Shaanxi Key Lab of Information Photonic Technique, Xi'an Jiaotong University, Xi'an 710049, China*

[2]*Department of Physics, University of Arkansas, Fayetteville, Arkansas 72701, USA and National Laboratory of Solid State Microstructures and Department of Physics, Nanjing University, Nanjing 210093, China*

Corresponding authors: a) wangrm@mail.xjtu.edu.cn; b) ypzhang@mail.xjtu.edu.cn

We report polarization dressed second-, fourth- and sixth-order fluorescence processes in a Pr^{3+}:Y_2SiO_5 crystal. By changing the polarization states of dressing fields and generating fields, the fluorescence baselines, suppression and Autler-Townes splitting of emission peaks can be controlled. The polarization dependences of fluorescence generated from two inequivalent crystallographic sites are compared. The experiment results agree with the dressing theoretical calculations well.

Keywords: fluorescence process, YSO crystal, polarization

I. INTRODUCTION

In recent decades, quantum coherence excitation and coherence transfer have been thoroughly studied in atomic gases. These processes lead to many important physical phenomena, such as electromagnetically induced transparency (EIT) [1], enhanced four-wave mixing (FWM) [2] and the group velocity control of traveling light [3, 4]. Compared with atomic gases, solid materials are more appropriate for practical applications. Rare-earth ion doped crystals (like Pr^{3+}:Y_2SiO_5) exhibit obvious advantages for coherent excitation, such as the absence of atomic diffusion, high density of atoms, compactness, long dephasing times and narrow homogeneous linewidths. The recent researches on quantum coherence control in rare-earth ion doped crystals have been reported, including EIT in solid materials [5, 6], enhanced FWM [7], stimulated Raman adiabatic passage [8], light velocity reduction and coherent storage [9,10], controllable erasing of optically stored information [11] and all-optical routing [12]. To realize practical applications, such processes are required to be controlled reliably.

Polarizations of the incident laser beams play important roles in atomic transitions when multi-Zeeman energy levels are involved in the atomic systems. The absorption and fluorescence

Physical Chemistry Chemical Physics Accepted Manuscript

spectra with different polarizations of probe and pump beams have been studied theoretically and experimentally [13, 14]. EIT processes can be controlled by selecting different transitions among Zeeman sublevels via the polarization states of the laser beams [15]. The polarization rotation of an optical beam also can be controlled by another stronger laser beam based on atomic coherence in multilevel EIT systems [16]. We have investigated the polarization dependences of FWM in atomic systems previously [17, 18]. The results show that the intensity and polarization characteristics of FWM signals can be effectively controlled by the polarization states of the pump and dressing beams.

The aim of this paper is to investigate the polarization dependences of fluorescence in Pr^{3+}:Y_2SiO_5 crystal. The two-level, V-type and Λ-type three-level, as well as N-type four-level systems are studied and compared. The polarization states of generating fields and dressing fields are modulated by a quarter-wave-plate (QWP) and a half-wave-plate (HWP). The dressing state theory is used to explain the experiment results. The paper is organized as follows: in Sec. II, we briefly introduce the experimental setup; in Sec. III, the theoretical model is discussed; in Sec. IV, we show the results and raise our explanation. Section V is our conclusion.

II. EXPERIMENTAL SETUP

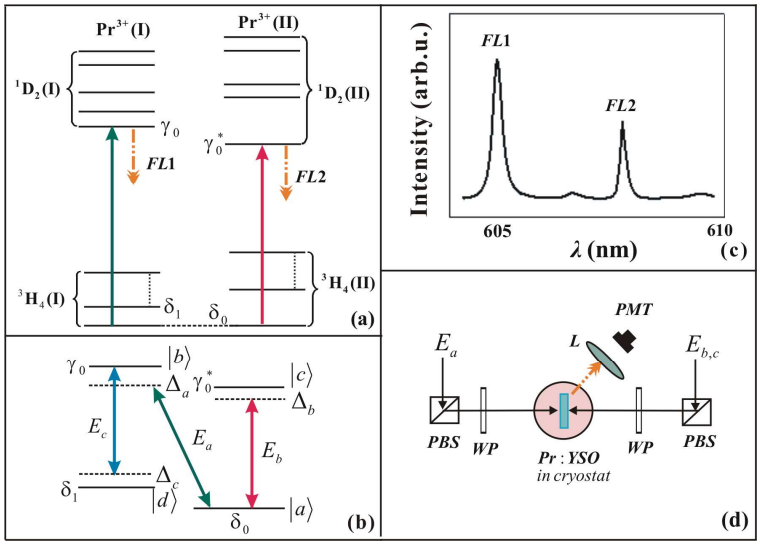

Figure 1 (color online). (a) Simplified energy-level diagram of Pr^{3+} ions in YSO crystal. (b) N-type four-level system ($|a\rangle\leftrightarrow|b\rangle\leftrightarrow|c\rangle\leftrightarrow|d\rangle$) for Pr^{3+} ion pairs. (c) Typical fluorescence signals in frequency domain. (d) Schematic diagram of the experimental arrangement.

Y_2SiO_5 is a monoclinic biaxial crystal and belongs to the C_{2h}^6 space group. When the Pr^{3+} ions substitute for the Y^{3+} ions in Y_2SiO_5 crystals they occupy two inequivalent crystallographic sites (sites I and II, respectively) [19]. The $^3H_4$, $^1D_2$ levels of Pr^{3+}:Y_2SiO_5 are split by the crystal field into manifolds consisting of nine and five singlets, respectively. Figure 1(a) shows the energy levels for the $^3H_4$ ground-state multiplets and $^1D_2$ excited-state multiplets for the two crystallographic sites of Pr^{3+} ions. These two crystallographic sites of Pr^{3+} ions have different Stark

Physical Chemistry Chemical Physics Accepted Manuscript

splittings, which can be identified by their fluorescence spectra (see Fig. 1 (c)). The spectral lines *FL*1 and *FL*2 are attributed to the optical transitions from the lowest Stark level γ_0 (γ_0^*) of $^1D_2$ to the lowest level δ_0 of the ground-state $^3H_4$ for sites I and II, respectively. In crystals, each Stark level is further split into three hyperfine states (±1/2, ±3/2, ±5/2) by the crystal field. The interaction between two optical centers with different electronic states can happen through phonon-assisted energy transfer [20]. In this case the donor-acceptor pairs consisting of Pr^{3+}(I) and Pr^{3+}(II) ions form. Moreover, the induced dipole-dipole interaction between Pr^{3+}(I) and Pr^{3+}(II) ions also happen, so one can treat the two ions as a heteronuclear-like molecule [21]. Depending on the interaction between Pr^{3+} ions, the multi-level systems are obtained (see Fig. 1 (b)).

Figure 1(d) shows the schematic diagram of the experimental arrangement. Our experiments are carried out in a 0.05 at % Pr^{3+} doped Y_2SiO_5 crystal. The sample (a 3-mm Pr^{3+}:Y_2SiO_5 crystal) is held at 77 K in a cryostat (CFM-102). Three tunable dye lasers (narrow scan with a 0.04 cm^{-1} linewidth) pumped by an injection locked single-mode Nd:YAG laser (Continuum Powerlite DLS 9010, 10 Hz repetition rate, 5 ns pulse width) are used to generate the pumping fields $\boldsymbol{E}_a$ (ω_a, Δ_a), $\boldsymbol{E}_b$ (ω_b, Δ_b), and $\boldsymbol{E}_c$ (ω_c, Δ_c) with the frequency detuning of $\Delta_i=\omega_{mn}-\omega_i$ (i=a, b, and c), where ω_{mn} denotes the corresponding atomic transition frequency. $\boldsymbol{E}_a$ drives the transition $|a\rangle\leftrightarrow|b\rangle$, $\boldsymbol{E}_b$ ($\boldsymbol{E}_c$) couples to the transition $|a\rangle\leftrightarrow|c\rangle$ ($|b\rangle\leftrightarrow|d\rangle$). The two-level system is formed when only one pumping field is on. With two pumping fields $\boldsymbol{E}_a$ and $\boldsymbol{E}_b$ (or $\boldsymbol{E}_c$) on, V-type three-level $|a\rangle\leftrightarrow|b\rangle\leftrightarrow|c\rangle$ (or Λ-type three-level system $|a\rangle\leftrightarrow|b\rangle\leftrightarrow|d\rangle$) is set up. When $\boldsymbol{E}_a$, $\boldsymbol{E}_b$ and $\boldsymbol{E}_c$ are all on, the N-type four-level system $|a\rangle\leftrightarrow|b\rangle\leftrightarrow|c\rangle\leftrightarrow|d\rangle$ is excited. The fluorescence signals are monitored by a photomultiplier tube (PMT) with a fast gated integrator. The HWP, QWP and polarized beam splitter (PBS) are used to control the polarization states of pumping fields.

III. THEORTICAL MODEL

A. Effective nonlinear susceptibilities

Classically, the fluorescence signal intensity is proportional to the square of the polarization induced in the medium. For the second-order fluorescence process, the polarization is $P_k^{(2)} = \varepsilon_0 \sum_{i,j} \chi^{(2)}_{ijk} | E_i || E_j |$. The Y_2SiO_5 crystal belongs to the C_{2h}^6 space group and considering that all the incident beams are transverse wave, only four tensor elements are nonzero which are denoted as $\chi^{(2)}_{xxy}$, $\chi^{(2)}_{xyx}$, $\chi^{(2)}_{yxx}$ and $\chi^{(2)}_{yyy}$. When HWPs are used to change the polarization directions of linear polarized incident beams, the effective nonlinear susceptibilities can be defined as

$$\chi_x = (\chi^{(2)}_{xyx} + \chi^{(2)}_{yxx}) \cos 2\theta \sin 2\theta , \quad (1a)$$

$$\chi_y = \chi^{(2)}_{xxy} \cos^2 2\theta + \chi^{(2)}_{yyy} \sin^2 2\theta , \quad (1b)$$

where θ is the rotated angle of the HWP's axis from the x axis. If the polarization states are changed by QWP, the effective nonlinear susceptibilities are

Physical Chemistry Chemical Physics Accepted Manuscript

$$\chi_x = (\chi^{(2)}_{xyx} + \chi^{(2)}_{yxx})\sqrt{\cos^4\theta + \sin^4\theta}\sqrt{2\left|\sin^2\theta\cos^2\theta\right|}\,, \tag{2a}$$

$$\chi_y = \chi^{(2)}_{xxy}(\cos^4\theta + \sin^4\theta) + 2\chi^{(2)}_{yyy}\sin^2\theta\cos^2\theta\,. \tag{2b}$$

B. Density matrix element

In quantum theory, the fluorescence signal intensity can also be described by the diagonal density matrix elements. In two-level system, with a strong pumping field $\boldsymbol{E}_a$ ($\boldsymbol{E}_b$) on, the fluorescence signal $FL1$ ($FL2$) is generated through the perturbation chains $\rho^{(0)}_{aa} \xrightarrow{\boldsymbol{E}_a} \rho^{(1)}_{ba} \xrightarrow{(\boldsymbol{E}_a)^*} \rho^{(2)}_{bb}$ and $\rho^{(0)}_{aa} \xrightarrow{(\boldsymbol{E}_a)^*} \rho^{(1)}_{ab} \xrightarrow{\boldsymbol{E}_a} \rho'^{(2)}_{bb}$ ($\rho^{(0)}_{aa} \xrightarrow{\boldsymbol{E}_b} \rho^{(1)}_{ca} \xrightarrow{(\boldsymbol{E}_b)^*} \rho^{(2)}_{cc}$ and $\rho^{(0)}_{aa} \xrightarrow{(\boldsymbol{E}_b)^*} \rho^{(1)}_{ca} \xrightarrow{\boldsymbol{E}_b} \rho'^{(2)}_{cc}$). Considering the self-dressing effect of $\boldsymbol{E}_a$ ($\boldsymbol{E}_b$), the diagonal density matrix element $\rho^{(2)}_{bb}$ ($\rho^{(2)}_{cc}$) is given by

$$\rho^{(2)}_{bb} = |G_a|^2/[(d_1 + |G_a|^2/\Gamma_{bb})(\Gamma_{bb} + |G_a|^2/d_1)], \tag{3a}$$

$$\rho^{(2)}_{cc} = |G_b|^2/[(d_2 + |G_b|^2/\Gamma_{bb})(\Gamma_{cc} + |G_b|^2/d_2)], \tag{3b}$$

where $d_1=\Gamma_{ba}+i\Delta_a$, $d_2=\Gamma_{ca}+i\Delta_b$, $G_i=-\mu_{ij}E_i/\hbar$ is the Rabi frequency of $\boldsymbol{E}_i$ with the electric dipole moment μ_{ij} between levels $|i\rangle$ and $|j\rangle$, and Γ_{ij} is the transverse decay rate. When the polarization direction of $\boldsymbol{E}_a$ is changed by a HWP, the diagonal density matrix element $\rho^{(2)}_{bb}$ can be described as

$$\begin{aligned}\rho^{(2)}_{FL1(x)} &= \rho^{(2)}_{bb(xyx)} + \rho^{(2)}_{bb(yxx)} \\ &= \frac{-2c_xc_y|G_a|^2\cos 2\theta\sin 2\theta}{[d_1 + |G_a|^2(c_y^2\cos^2 2\theta + c_x^2\sin^2 2\theta)/\Gamma_{bb}][\Gamma_{bb} + |G_a|^2(c_y^2\cos^2 2\theta + c_x^2\sin^2 2\theta)/d_1]},\end{aligned} \tag{4a}$$

$$\begin{aligned}\rho^{(2)}_{FL1(y)} &= \rho^{(2)}_{bb(xxy)} + \rho^{(2)}_{bb(yyy)} \\ &= \frac{-c_x^2|G_a|^2\cos^2 2\theta}{(d_1 + c_x^2|G_a|^2\cos^2 2\theta/\Gamma_{bb})(\Gamma_{bb} + c_x^2|G_a|^2\cos^2 2\theta/d_1)}\,, \\ &\quad + \frac{-c_y^2|G_a|^2\sin^2 2\theta}{(d_1 + c_y^2|G_a|^2\sin^2 2\theta/\Gamma_{bb})(\Gamma_{bb} + c_y^2|G_a|^2\sin^2 2\theta/d_1)}\end{aligned} \tag{4b}$$

where $c_{x,y}$ is the anisotropic factor denoting the different susceptibilities $\chi^{(2)}_{xxy}$, $\chi^{(2)}_{yyy}$ in different directions.

In V-type three-level system, when two pumping fields $\boldsymbol{E}_a$ and $\boldsymbol{E}_b$ are both on, two fluorescence signals $FL1$ and $FL2$ are generated simultaneously. The intensity of the total fluorescence signals is the sum of two signals. Moreover, these two processes can interplay with each other. Considering the coherence of the system, such process can be described by the fourth-order coherence process as

Physical Chemistry Chemical Physics Accepted Manuscript

$$\rho_{bb}^{(4)}=\frac{-|G_b|^2}{\left(d_2+|G_b|^2/\Gamma_{cc}+|G_a|^2/d_{21}\right)\left(\Gamma_{aa}+|G_a|^2/d_1+|G_b|^2/d_2\right)}\times\frac{-|G_a|^2}{\left(d_1+|G_a|^2/\Gamma_{bb}+|G_b|^2/d_{12}\right)\left(\Gamma_{bb}+|G_a|^2/d_1\right)} \quad (5a)$$

$$\rho_{cc}^{(4)}=\frac{-|G_a|^2}{\left(d_1+|G_a|^2/\Gamma_{bb}+|G_b|^2/d_{12}\right)\left(\Gamma_{aa}+|G_a|^2/d_1+|G_b|^2/d_2\right)}\times\frac{-|G_b|^2}{\left(d_2+|G_b|^2/\Gamma_{cc}+|G_a|^2/d_{21}\right)\left(\Gamma_{cc}+|G_b|^2/d_2\right)} \quad (5b)$$

where $d_{12}=\Gamma_{bc}+i(\Delta_a-\Delta_b)$, $d_{21}=\Gamma_{cb}+i(\Delta_b-\Delta_a)$. When the polarization state of $\boldsymbol{E}_a$ is changed from linearly polarized beam into circularly polarized beam by a QWP, different polarized beams can excite different transition paths among Zeeman sublevels. In this case, Clebsch-Gordan (CG) coefficients associated with the various transition paths play an important role for calculating the intensities of fluorescence, since it makes the electric dipole moment μ_{ij} and Rabi frequencies G_i different. Figure 2 shows transition paths and CG coefficients at different laser polarization states. The total fluorescence signals are the summing contribution of each transition path. When $\boldsymbol{E}_a$ is linearly polarized, only $|a_j\rangle\leftrightarrow|b_j\rangle$ (j=±1/2, ±3/2, ±5/2) vertical transition pathways are allowed. Although there are several perturbation chains for the generated nonlinear signal, it is reasonable to choose one of them to analyze the physical mechanism. For example, the diagonal density matrix element for $|a_{5/2}\rangle\leftrightarrow|b_{5/2}\rangle$ transition pathway can be written as

$$\rho_{b5/2b5/2}^{(4)}=\frac{|G_{b5/2}|^2}{[\Gamma_{c5/2a5/2}+i\Delta_b+\frac{|G_{b5/2}|^2}{\Gamma_{c5/2c5/2}}+\frac{|G^0_{a5/2}|^2}{\Gamma_{c5/2b5/2}+i(\Delta_b-\Delta_a)}](\Gamma_{a5/2a5/2}+\frac{|G_{b5/2}|^2}{\Gamma_{c5/2a5/2}+i\Delta_b}+\frac{|G^0_{a5/2}|^2}{\Gamma_{b5/2a5/2}+i\Delta_a})}\times\frac{-|G^0_{a5/2}|^2}{[\Gamma_{b5/2a5/2}+i\Delta_a+\frac{|G^0_{a5/2}|^2}{\Gamma_{b5/2b5/2}}+\frac{|G_{b5/2}|^2}{\Gamma_{b5/2c5/2}+i(\Delta_a-\Delta_b)}](\Gamma_{b5/2b5/2}+\frac{|G^0_{a5/2}|^2}{\Gamma_{b5/2a5/2}+i\Delta_a})} \quad (6a)$$

The left-circularly and right-circularly polarized beams drive the transitions $|a_{j+1}\rangle\leftrightarrow|b_j\rangle$ and $|a_j\rangle\leftrightarrow|b_{j+1}\rangle$, respectively. The density matrix elements corresponding to $|a_{5/2}\rangle\leftrightarrow|b_{3/2}\rangle$ and $|a_{-5/2}\rangle\leftrightarrow|b_{-3/2}\rangle$ are

$$\rho_{b3/2b3/2}^{(4)}=\frac{|G_{b5/2}|^2}{[\Gamma_{c5/2a5/2}+i\Delta_b+\frac{|G_{b5/2}|^2}{\Gamma_{c5/2c5/2}}+\frac{|G^-_{a5/2}|^2}{\Gamma_{c5/2b3/2}+i(\Delta_b-\Delta_a)}](\Gamma_{a5/2a5/2}+\frac{|G^-_{a5/2}|^2}{\Gamma_{b3/2a5/2}+i\Delta_a}+\frac{|G_{b5/2}|^2}{\Gamma_{c5/2a5/2}+i\Delta_b})}\times\frac{-|G^-_{a5/2}|^2}{[\Gamma_{b3/2a5/2}+i\Delta_a+\frac{|G^-_{a5/2}|^2}{\Gamma_{b3/2b3/2}}+\frac{|G_{b5/2}|^2}{\Gamma_{b3/2c5/2}+i(\Delta_a-\Delta_b)}](\Gamma_{b3/2b3/2}+\frac{|G^-_{a5/2}|^2}{\Gamma_{b3/2a5/2}+i\Delta_a}+\frac{|G_{b5/2}|^2}{\Gamma_{c5/2a5/2}+i\Delta_b})} \quad (6b)$$

$$\rho_{b-3/2b-3/2}^{(4)}=\frac{|G_{b-5/2}|^2}{[\Gamma_{c-5/2a-5/2}+i\Delta_b+\frac{|G_{b-5/2}|^2}{\Gamma_{c-5/2c-5/2}}+\frac{|G^+_{a-5/2}|^2}{\Gamma_{c-5/2b-3/2}+i(\Delta_b-\Delta_a)}](\Gamma_{a-5/2a-5/2}+\frac{|G^+_{a-5/2}|^2}{\Gamma_{b-3/2a-5/2}+i\Delta_a}+\frac{|G_{b-5/2}|^2}{\Gamma_{c-5/2a-5/2}+i\Delta_b})}\times\frac{-|G^+_{a-5/2}|^2}{[\Gamma_{b-3/2a-5/2}+i\Delta_a+\frac{|G^+_{a-5/2}|^2}{\Gamma_{b-3/2b-3/2}}+\frac{|G_{b-5/2}|^2}{\Gamma_{b-3/2c-5/2}+i(\Delta_a-\Delta_b)}](\Gamma_{b-3/2b-3/2}+\frac{|G^+_{a-5/2}|^2}{\Gamma_{b-3/2a-5/2}+i\Delta_a})} \quad (6c)$$

Physical Chemistry Chemical Physics Accepted Manuscript

where G_i^0, G_i^- and G_i^+ are the Rabi frequencies for linearly, left- and right-circularly polarized beams, respectively. So it will show different transition strengths induced by different Rabi frequencies in Zeeman sublevels.

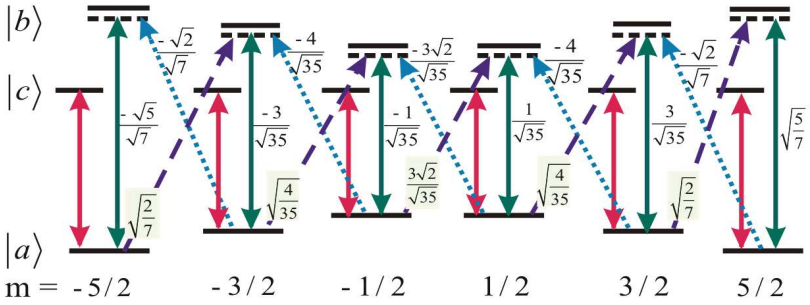

Figure 2 (color online). Zeeman energy levels and transition paths at different polarization states. Solid lines: transitions for the linearly polarized beam; dotted lines: transitions for the left circularly polarized beam; dashed lines: transitions for the right circularly polarized beam.

In Λ-type three-level system, when the polarization direction of $\boldsymbol{E}_c$ is changed by HWP, the modulated fluorescence signal $FL1$ is generated. The density matrix elements also can be described by the fourth-order coherence process.

$$\rho_{bb(xxxxy)}^{(4)} = \frac{c_x^2 |G_a|^2 |G_c|^2 \cos^2 2\theta_3}{\left(d_1 + |G_a|^2/\Gamma_{bb} + c_x^2 |G_c|^2 \cos^2 2\theta_3 / d_{31}\right)} \frac{1}{\left(d_3 + c_x^2 |G_c|^2 \cos^2 2\theta_3/\Gamma_{bb} + |G_a|^2/d_{13}\right)\left(\Gamma_{bb} + c_x^2 |G_c|^2 \cos^2 2\theta_3/d_3 + |G_a|^2/d_1\right)^2}, \quad (7a)$$

$$\rho_{bb(xxyyy)}^{(4)} = \frac{c_y^2 |G_a|^2 |G_c|^2 \sin^2 2\theta_3}{\left(d_1 + |G_a|^2/\Gamma_{bb} + c_y^2 |G_c|^2 \sin^2 2\theta_3 / d_{31}\right)} \frac{1}{\left(d_3 + c_y^2 |G_c|^2 \sin^2 2\theta_3/\Gamma_{bb} + |G_a|^2/d_{13}\right)\left(\Gamma_{bb} + c_y^2 |G_c|^2 \sin^2 2\theta_3/d_3 + |G_a|^2/d_1\right)^2}, \quad (7b)$$

where $d_3=\Gamma_{da}+i\Delta_c$, $d_{31}=\Gamma_{bd}+i(\Delta_a-\Delta_c)$, $d_{13}=\Gamma_{db}+i(\Delta_c-\Delta_a)$. In N-type four-level system with three pumping fields $\boldsymbol{E}_a$, $\boldsymbol{E}_b$ and $\boldsymbol{E}_c$, multi-dressed fluorescence signals can be obtained. Such multi-dressed fluorescence signals can be described by sixth-order coherence process as

$$\rho_{bb}^{(6)} = \frac{-|G_c|^2 |G_a|^2 |G_b|^2}{[d_3 + |G_c|^2/\Gamma_{dd} + |G_a|^2/(d_{13} + |G_b|^2/d_{23})](\Gamma_{bb} + |G_c|^2/d_3 + A)} \times \frac{1}{\left(d_1 + |G_a|^2/\Gamma_{aa} + |G_c|^2/d_{31} + |G_b|^2/d_{12}\right)(\Gamma_{aa} + |G_b|^2/d_2 + A)} \times \frac{1}{\left(d_2 + |G_b|^2/\Gamma_{cc} + |G_a|^2/d_{21}\right)\left(\Gamma_{cc} + |G_b|^2/d_2\right)}, \quad (8)$$

where $d_{23}=\Gamma_{bd}+i(\Delta_c-\Delta_a+\Delta_b)$, $A=|G_a|^2/(d_1+|G_c|^2/d_{31})$.

IV. RESULTS AND DISCUSSION

Physical Chemistry Chemical Physics Accepted Manuscript

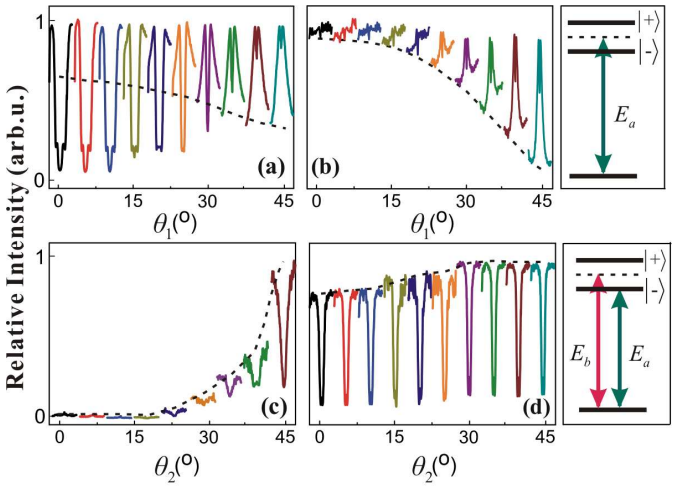

Figure 3 (color online). Dependence of the relative intensity of fluorescence on the rotation angle of the HWP in two-level system. (a) Fluorescence signals *FL*1 and (b) *FL*2 with one pumping field. (c) Fluorescence signals *FL*1 and (d) *FL*2 with two pumping fields.

First, we investigate the fluorescence signal in the two-level system. Figures 3(a) and 3(b) show the signals *FL*1 ($|a\rangle\leftrightarrow|b\rangle$) and *FL*2 ($|a\rangle\leftrightarrow|c\rangle$) at different polarization directions with one pumping field $\boldsymbol{E}_a$, respectively. Each fluorescence curve shows the Autler-Townes-like (AT) splitting that caused by the saturation absorption effect of the strong beam $\boldsymbol{E}_a$. The self-dressing effect of $\boldsymbol{E}_a$ on spectra splitting is reflected by $|G_a|^2/d_1$ (see Eq. (3)). In Fig. 3(a), with the rotation angle of the HWP changing from 0^o to 45^o (the dressing term changes from $c_x^2|G_a|^2/d_1$ to $c_y^2|G_a|^2/d_1$ in Eq. (4b)), the depth and width of the suppressed dip reduces, and the fluorescence emission peaks increase gradually. It is mean that the dressing effect of $\boldsymbol{E}_a$ is greater at 0^o (horizontal polarization) than that at 45^o (vertical polarization). The baseline of each signal which is the non-resonant fluorescence signal also reduces with the rotation angle increasing. It can be interpreted by the change of numerator from $c_x^2|G_a|^2$ to $c_y^2|G_a|^2$ in Eq. (4b). In this case, the strong field $\boldsymbol{E}_a$ acts as the dressing field and the generating field simultaneously. For *FL*2 (Fig. 3(b)), the evolution of the baseline is as same as *FL*1, but the variation of the AT splitting is unapparent at different polarization directions. It indicates that the level splitting of γ_0^* (sites II) is insensitive to polarization direction of the dressing field. Sites I and II are two inequivalent crystallographic sites. Figures 3(c) and 3(d) are the signals *FL*1 and *FL*2 with two pumping fields, respectively. The dressing field $\boldsymbol{E}_b$ is resonant with relevant transitions (satisfies the suppression condition Δ_b=0), while the frequency detuning of the generating field $\boldsymbol{E}_a$ is scanned. The polarization direction of $\boldsymbol{E}_b$ is changed by HWP. One can see that the fluorescence baselines for both *FL*1 and *FL*2 are increase with the rotation angle θ_2 of HWP. Compared with the case pumped by one field (Fig. 3(b)), the suppressed dip of *FL*2 with two pumping fields becomes more obvious and the fluorescence emission peaks disappear. This attributes to the external-dressing effect of $\boldsymbol{E}_b$. The coupling between the strong field $\boldsymbol{E}_b$ and particles leads to the generation of dark state, and the

Physical Chemistry Chemical Physics Accepted Manuscript

external-dressing splitting ($|G_b|^2/d_{02}$) overlaps with the self-dressing splitting ($|G_a|^2/d_1$). In this case, the Eq. (4b) is rewritten as

$$\rho^{(2)}_{FL1(y)} = \rho^{(2)}_{bb(xxy)} + \rho^{(2)}_{bb(yyy)}$$
$$= \frac{-|G_a|^2}{(d_1+|G_a|^2/\Gamma_{bb}+c_x^2|G_b|^2\cos^2 2\theta_2/d_{02})(\Gamma_{bb}+|G_a|^2/d_1+c_x^2|G_b|^2\cos^2 2\theta_2/d_2')} + \frac{-|G_a|^2}{(d_1+|G_a|^2/\Gamma_{bb}+c_y^2|G_b|^2\sin^2 2\theta_2/d_{02})(\Gamma_{bb}+|G_a|^2/d_1+c_y^2|G_b|^2\sin^2 2\theta_2/d_2')} \quad , (9)$$

where $d'_2=\Gamma_{ba}+i\Delta_b$ and $d_{02}=\Gamma_{bb}+i(\Delta_a-\Delta_b)$. Because the polarization direction of the external-dressing field is changed, the intensity of the fluorescence baseline depends on the dressing term $c_x^2|G_b|^2\cos^2 2\theta_2/d_2'$ of $\boldsymbol{E}_b$. We can see the suppression effect of $\boldsymbol{E}_b$ on the fluorescence baseline is greater at 0^o ($c_x^2|G_b|^2/d_2'$) than that at 45^o ($c_y^2|G_b|^2/d_2'$). For *FL*1, the baseline is suppressed even to zero at 0^o, but the suppression effect on the baseline of *FL*2 is smaller than *FL*1. We can draw the conclusion that polarization dependences for *FL*1 and *FL*2 are different. Such difference results from the crystallographic aeolotropy of Y_2SiO_5 crystal.

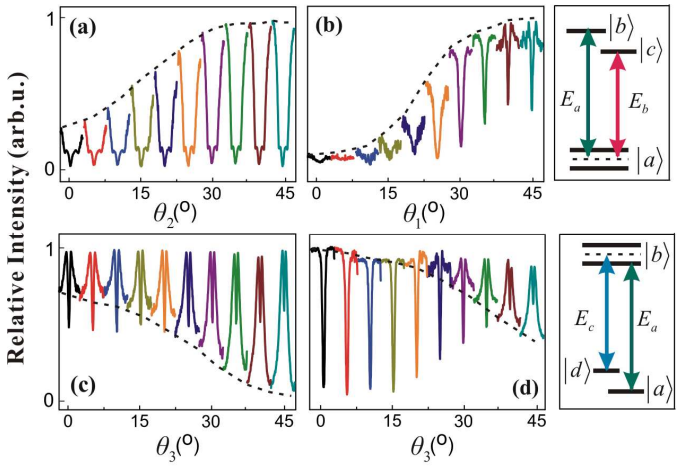

Figure 4 (color online). (a) Fluorescence signals *FL*1 and (b) *FL*2 in V-type three-level systems when the dressing fields $\boldsymbol{E}_b$ and $\boldsymbol{E}_a$ are changed by HWP, respectively. (c) Fluorescence signals *FL*1 in Λ-type three-level and (d) *FL*1 in N-type four-level systems when the dressing field $\boldsymbol{E}_c$ is changed by HWP.

Now, we investigate the fluorescence signal in the V-type three-level system (Figs. 4(a) and 4(b)). In this case, the intensity of the fluorescence baseline is the sum of two signals *FL*1 and *FL*2, so the measured results are the combinative action of dressing and excitation effects. The AT splitting results from the dressing effects of $\boldsymbol{E}_a$ ($|G_a|^2/d_1$) and $\boldsymbol{E}_b$ ($|G_b|^2/d_2$) on the level $|a\rangle$. For *FL*1 (Figs. 4(a)), the fluorescence baseline raises as the dressing field $\boldsymbol{E}_b$ is changed from horizontally to vertically polarized, which can be interpreted by different dressing effects of $\boldsymbol{E}_b$ (changing from $c_x^2|G_b|^2/\Gamma_{cc}$ to $c_y^2|G_b|^2/\Gamma_{cc}$). However, compared with two-level system, the fluorescence

Physical Chemistry Chemical Physics Accepted Manuscript

baseline is not suppressed to zero at 0°. It is due to the generation of fluorescence *FL*2 from level $|c\rangle$. The width of the suppressed dip reduces gradually with θ_2 but the depth does not change. For *FL*2 (Figs. 4(b)), the suppression effect of dressing field $\boldsymbol{E}_a$ at 0° is greater than that in two-level system, and the depth of the suppressed dip reduces gradually with θ_1. This is because the dressing effect of $\boldsymbol{E}_a$ is sensitive to the polarization.

Figure 4(c) shows the signal *FL*1 in Λ-type three-level system and the polarization direction of the dressing field $\boldsymbol{E}_c$ is changed by HWP. It is different from the V-type three-level system that the baseline reduces gradually with θ_3, and the fluorescence emission peaks become obviously. As described in Eq. (7), these phenomena can be interpreted by the cooperation of the numerator $c_x^2 |G_c|^2 \cos^2 2\theta_3$ and the dressing term $c_x^2 |G_c|^2 \cos^2 2\theta_3 / \Gamma_{bb}$. The AT splitting of emission peaks is attributed to the dressing effects of $\boldsymbol{E}_a$ ($|G_a|^2 / d_1$) and $\boldsymbol{E}_c$ ($c_x^2 |G_c|^2 \cos^2 2\theta_3 / d_{31}$) on level $|b\rangle$. When three fields $\boldsymbol{E}_a$, $\boldsymbol{E}_b$ and $\boldsymbol{E}_c$ are all on, a N-type four-level system is set up. We keep the dressing fields $\boldsymbol{E}_b$ and $\boldsymbol{E}_c$ close to the resonant point and scan the detuning of the generating field $\boldsymbol{E}_a$. One can see in Fig. 4 (d), the baseline is greater than which in Λ-type three-level. It is due to the generation of fluorescence *FL*2 by $\boldsymbol{E}_b$. There is excitation competition on the particles of ground state between $\boldsymbol{E}_a$ and $\boldsymbol{E}_b$. Because of the further dressing by $\boldsymbol{E}_b$, the emission peaks of *FL*1 reduce and the suppressed dips become deeper.

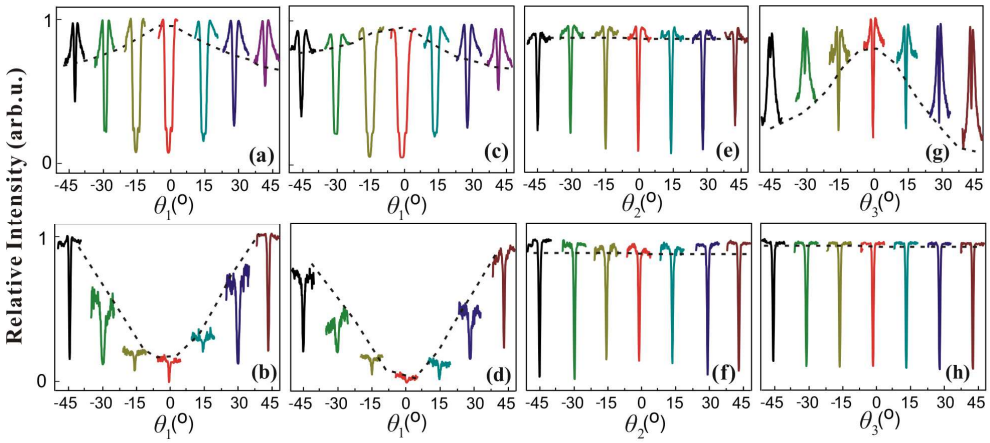

Figure 5 (color online). (a) Fluorescence signals *FL*1 and (b) *FL*2 in V-type three-level systems when $\boldsymbol{E}_a$ is changed by QWP. (c) Fluorescence signals *FL*1 and (d) *FL*2 in N-type four-level systems when $\boldsymbol{E}_a$ is changed by QWP. (e) Fluorescence signals *FL*1 and (f) *FL*2 in N-type four-level systems when $\boldsymbol{E}_b$ is changed by QWP. (g) Fluorescence signals *FL*1 and (h) *FL*2 in N-type four-level systems when $\boldsymbol{E}_c$ is changed by QWP.

Next, we use a QWP to modulate the polarization states of pumping fields. Figures 5(a) and 5(b) illustrate the fluorescence signals *FL*1 and *FL*2 in a V-type three-level system when the field $\boldsymbol{E}_a$ is changed by QWP, respectively. For *FL*1, when the polarization state of $\boldsymbol{E}_a$ changes from left-circularly polarized to linearly polarized, and then to right-circularly polarized (the QWP

Physical Chemistry Chemical Physics Accepted Manuscript

rotating from −45° to 0° and then to 45°), we can see both fluorescence baseline and AT splitting evolve from weak to strong and then to weak. Figure 2 shows transition paths and CG coefficients at different laser polarization states. Although there are several transition paths for the generated fluorescence signal, considering the population of each level, the optical transition from the lowest crystal-field level $|\pm 5/2\rangle$ is the dominant one. Since $\boldsymbol{E}_a$ is not only the dressing field but also the generating field for *FL*1, we should simultaneously consider the self-dressing role and generating role. Because the Rabi frequency $G^0_{a\pm 5/2}$ for linearly polarized state is greater than $G^-_{a5/2}$ ($G^+_{a-5/2}$) for left- (right-) circularly polarized state, so the baseline (decided by $|G^0_{a5/2}|^2$ in numerator of Eq. 6(a)) and AT splitting (decided by $|G^0_{a5/2}|^2/(\Gamma_{b5/2a5/2}+i\Delta_a)$) are stronger at 0° than that at ±45°. For *FL*2, $\boldsymbol{E}_a$ mainly acts as a dressing field. The suppressed effect of linearly polarized field $|G^0_{a5/2}|^2/\Gamma_{b5/2b5/2}$ is stronger than left- ($|G^-_{a5/2}|^2/\Gamma_{b3/2b3/2}$) and right-circularly ($|G^+_{a-5/2}|^2/\Gamma_{b-3/2b-3/2}$) polarized field, so the lowest fluorescence baseline occurs at θ_1=0°.

Figures 5(c)-5(h) show the fluorescence signals in N-type four-level systems. When the polarization state of $\boldsymbol{E}_a$ is modulated (shown in Figs. 5(c) and 5(d)), the evolvement of the fluorescence baseline and suppressed dips is as similar as which in V-type three-level, but the signals are further suppressed by the multi-dressing effect of $\boldsymbol{E}_c$ ($|G_c|^2/\Gamma_{dd}$) and $\boldsymbol{E}_b$ ($|G_b|^2/\Gamma_{cc}$). When the polarization state of $\boldsymbol{E}_b$ is modulated by QWP, both fluorescence signals *FL*1 (Fig. 5(e)) and *FL*2 (Fig. 5(f)) show a little change on the rotation angle θ_2. This means that the level of site II is insensitive to the polarization state of pumping field. Figures 5(g) and 5(h) show signals *FL*1 and *FL*2, respectively, as the dressing field $\boldsymbol{E}_c$ is modulated by QWP. According to Eq. (8), the dressing effect of $\boldsymbol{E}_c$ on level $|b\rangle$ of *FL*1 is determined by $|G_c|^2/d_{31}$. The Rabi frequency of linearly polarized field is greater than circularly polarized field, so the AT splitting at 0° is stronger than that at ±45°. On the other hand, $\boldsymbol{E}_c$ also acts as a generating field for *FL*1, so the baseline excited by G^0_c at 0° is greater than that excited by $G^{\pm}_c$ at ±45°. In Fig. 5(h), one can see the fluorescence signal *FL*2 doesn't change with the rotation angle θ_3. This is because $\boldsymbol{E}_c$ does not dress the level $|a\rangle$ and $|c\rangle$ of *FL*2. For *FL*2, it is mainly dressed by $\boldsymbol{E}_a$.

V. CONCLUSION

In summary, we have reported the polarization dependences of fluorescence signals in two-level, V-type and Λ-type three-level, as well as N-type four-level systems of Pr^{3+}:Y_2SiO_5 crystal. The suppressed dips, emission peaks and fluorescence baselines show different evolvements as the polarization states of generating fields and dressing fields are changed by QWP or HWP. For the level of site I, the dressing effects of horizontal and linearly polarized fields are greater than that of vertical and circularly polarized fields. However, the dressing effect on the level of site II is insensitive to the polarization state. Our experiment data are in good agreements with the theoretical results from dressing effect analysis. Furthermore, our results provide an

Physical Chemistry Chemical Physics Accepted Manuscript

effective method to control high-order fluorescence processes.

Acknowledgement

This work was supported by the 973 Program (2012CB921804), KSTIT (2014KCT-10), NSFC (11104214, 61108017, 11104216, 61205112), KLPSP (2013SZS04-Z02), FRFCU (xjj2014099), and XJTUIT (cxtd2014003).

References

[1] Xiao, M.; Li, Y. Q.; Jin, S. Z.; Gea-Banacloche, J. Measurement of dispersive properties of electromagnetically induced transparency in rubidium atoms. *Phys. Rev. Lett.* **1995**, 74, 666-669.

[2] Li, C. B.; Zheng, H. B.; Zhang, Y. P.; Nie, Z. Q.; Song, J. P.; Xiao, M. Observation of enhancement and suppression in four-wave mixing processes. *Appl. Phys. Lett.* **2009**, 95, 041103.

[3] Hau, L. V.; Harris, S. E.; Dutton, Z.; Behroozi, C. H. Light speed reduction to 17 meters per second inan ultracold atomic gas. *Nature* **1999**, 397, 594-598.

[4] Liu, C.; Dutton, Z.; Behroozi, C. H.; Hau, L. V. Observation of coherent optical information storage in an atomic medium using halted light pulses. *Nature* **2001**, 409, 490-493.

[5]Ham, B.; Hemmer, P.; Shahriar, M. Efficient electromagnetically induced transparency in a rare-earth doped crystal. *Opt. Commun.* **1997**, 144, 227-230.

[6] Wei, C.; Manson, N. Observation of electromagnetically induced transparency within an electron spin resonance transition. *J. Opt. B* **1999**, 1, 464-468.

[7] Wang, H. H.; Li, A. J.; Du, D. M.; Fan, Y. F.; Wang, L.; Kang, Z. H.; Jiang, Y.; Wu, J. H.; Gao, J. Y. Enhanced four-wave mixing by atomic coherence in a Pr^{3+}:Y_2SiO_5 crystal. *Appl. Phys. Lett.* **2008**, 93, 221107.

[8] Klein, J.; Beil, F.; Halfmann, T.; Robust population transfer by stimulated Raman adiabatic passage in a Pr^{3+}:Y_2SiO_5 crystal. *Phys. Rev. Lett.* **2007**, 99, 113003.

[9] Longdell, J. J.; Fraval, E.; Sellars, M. J.; Manson, N. B. Stopped light with storage times greater than one second using electromagnetically induced transparency in a solid. *Phys. Rev. Lett.* **2005**, 95, 063601.

[10] Wang, H. H.; Fan, Y. F.; Wang, R.; Wang, L.; Du, D. M.; Kang, Z. H.; Jiang, Y.; Wu, J. H.; Gao, J. Y. Slowing and storage of double light pulses in a Pr^{3+}:Y_2SiO_5 crystal. *Opt. Lett.* **2009**, 34, 2596-2598.

[11] Wang, H.; Kang, Z.; Jiang, Y.; Li, Y.; Du, D.; Wei, X.; Wu, J.; Gao, J. Erasure of stored optical information in a Pr^{3+}:Y_2SiO_5 crystal. *Appl. Phys. Lett.* **2008**, 92, 011105.

[12] Wang, H.; Li, A.; Du, D.; Fan, Y.; Wang, ; Kang, Z.; Jiang, Y.; Wu, J.; Gao, J. All-optical routing by light storage in a Pr^{3+}:Y_2SiO_5 crystal. *Appl. Phys. Lett.* **2008**, 93, 221112.

[13] Lipsich, A.; Barreiro, S.; Akulshin, A. M.; Lezama, A. Absorption spectra of driven degenerate two-level atomic systems. *Phys. Rev. A* **2000**, 61, 053803.

[14] Milner, V.; Prior, Y. Multilevel dark states: Coherent population trapping with elliptically polarized incoherent light. *Phys. Rev. Lett.* **1998**, 80, 940.

[15] Wang, B.; Xiao, Y. J.; Yang, X.; Xie, C.; Wang, H.; Xiao, M. Multi-dark-state resonances in

Physical Chemistry Chemical Physics Accepted Manuscript

cold multi-Zeeman-sublevel atoms. *Opt. Lett.* **2006**, 31, 3647-3649.

[16] Li, S. J.; Wang, B.; Yang, X. D.; Han, Y. X.; Wang, H.; Xiao M.; Peng, K. C. Controlled polarization rotation of an optical field in multi-Zeeman-sublevel atoms. *Phys. Rev. A* **2006**, 74, 033821.

[17] Wang, R.M.; Wu, Z. K.; Sang, S. L.; Song, J. P.; Zheng, H. B.; Wang, Z. G.; Li, C. B.; Zhang, Y. P. Coexisting polarized four-wave mixing processes in a two-level atomic system. *J. Opt. Soc. Am. B* **2011**, 28, 2940-2946.

[18] Wang, R. M.; Du, Y.G.; Zhang, Y.P.; Zheng, H.B.; Nie, Z. Q.; Li, C. B.; Li, Y. Y.; Song, J. P.; Xiao, M. Polarization spectroscopy of dressed four-wave mixing in three-level atomic system. *J. Opt. Soc. Am. B* **2009**, 26, 1710-1719.

[19] Equall, R. W.; Cone, R. L.; Macfarlane, R. M. Homogenous broadening and hyperfine structure of optical transitions in Pr^{3+}:Y_2SiO_5. *Phys. Rev. B* **1995,** 52, 3963-3969.

[20] Zhmurin, P. N.; Zhnamenski, N. V.; Yurkina, T. G.; Malyukin, Yu. V. Strong quenching of Y_2SiO_5: Pr^{3+} nanocrystal luminescence by praseodymium nonuniform distribution. *Phys. Stat. Sol.* (*b*). **2007**, 244, 3325-3332.

[21] Li, C.B.; Wang L.L.; Zheng H.B.; Lan H.Y.; Lei C.J.; Zhang D.; Xiao M.; Zhang Y.P. All-optically controlled fourth- and sixth-order fluorescence processes of Pr^{3+}:YSO. *Appl. Phys. Lett.* **2014**,104, 051912.

Physical Chemistry Chemical Physics Accepted Manuscript

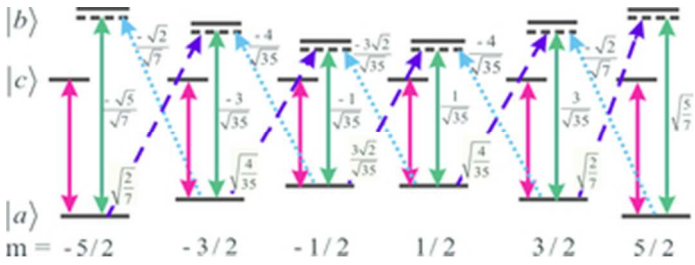

29x10mm (300 x 300 DPI)

Physical Chemistry Chemical Physics Accepted Manuscript